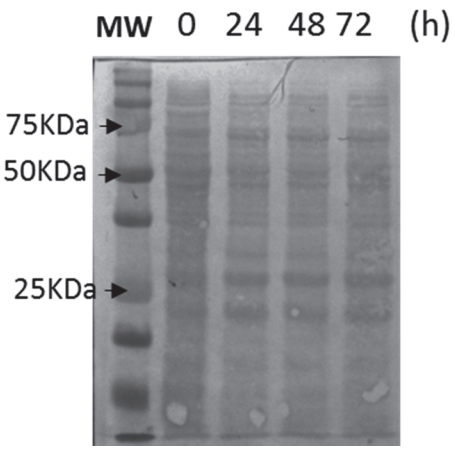

Supplemental Figure S1: Total protein profiles during sulfur starvation.

Protein degradation was assessed in total protein extracts of WT-S24 cells starved in TAP-S under low light over 72 h, harvested at the time points indicated and stained with Ponceau red on nitrocellulose membrane.

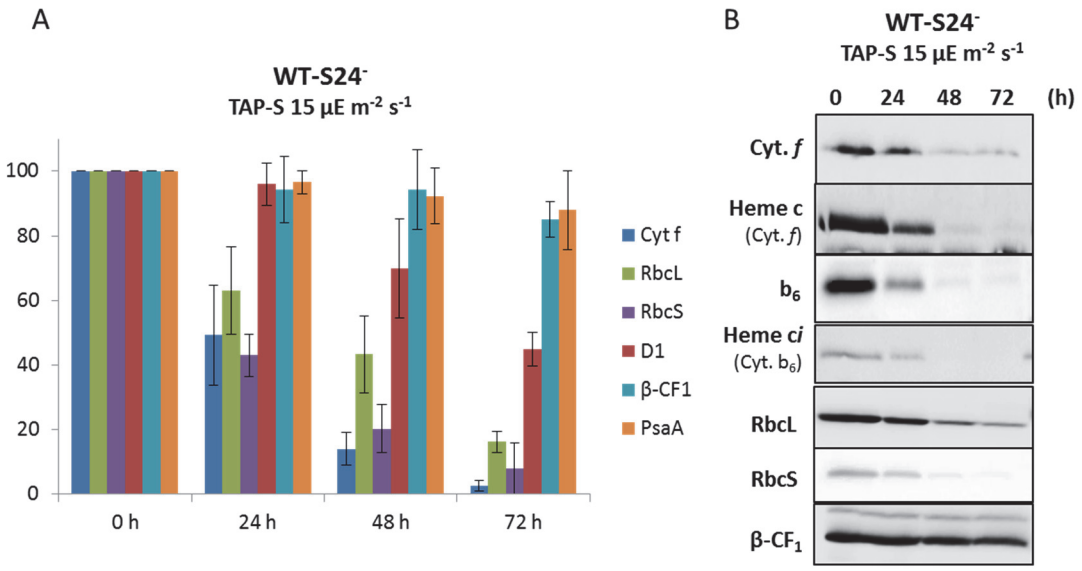

Supplemental Figure S2. Photosynthetic complex accumulation upon sulfur starvation and interconnection between cytochrome *b*$_6$*f* degradation and inactivation.

(A) Relative band intensity of the indicated antibodies in WT-S24$^-$ cells starved in TAP-S medium at 15 µE m^{-2} s^{-1}. Data show the mean of three independent experiments ± SEM, values are normalized to 100 % for T_0.

(B) Whole protein extracts from WT-S24$^-$ cells starved in TAP-S at 15 µE m^{-2} s^{-1}, harvested at the time points indicated and probed with the antibodies indicated. Heme peroxidase activity was detected using enhanced chemiluminescence (ECL). β-CF$_1$ is an internal loading control. Samples were loaded at least three times on mirror gels.

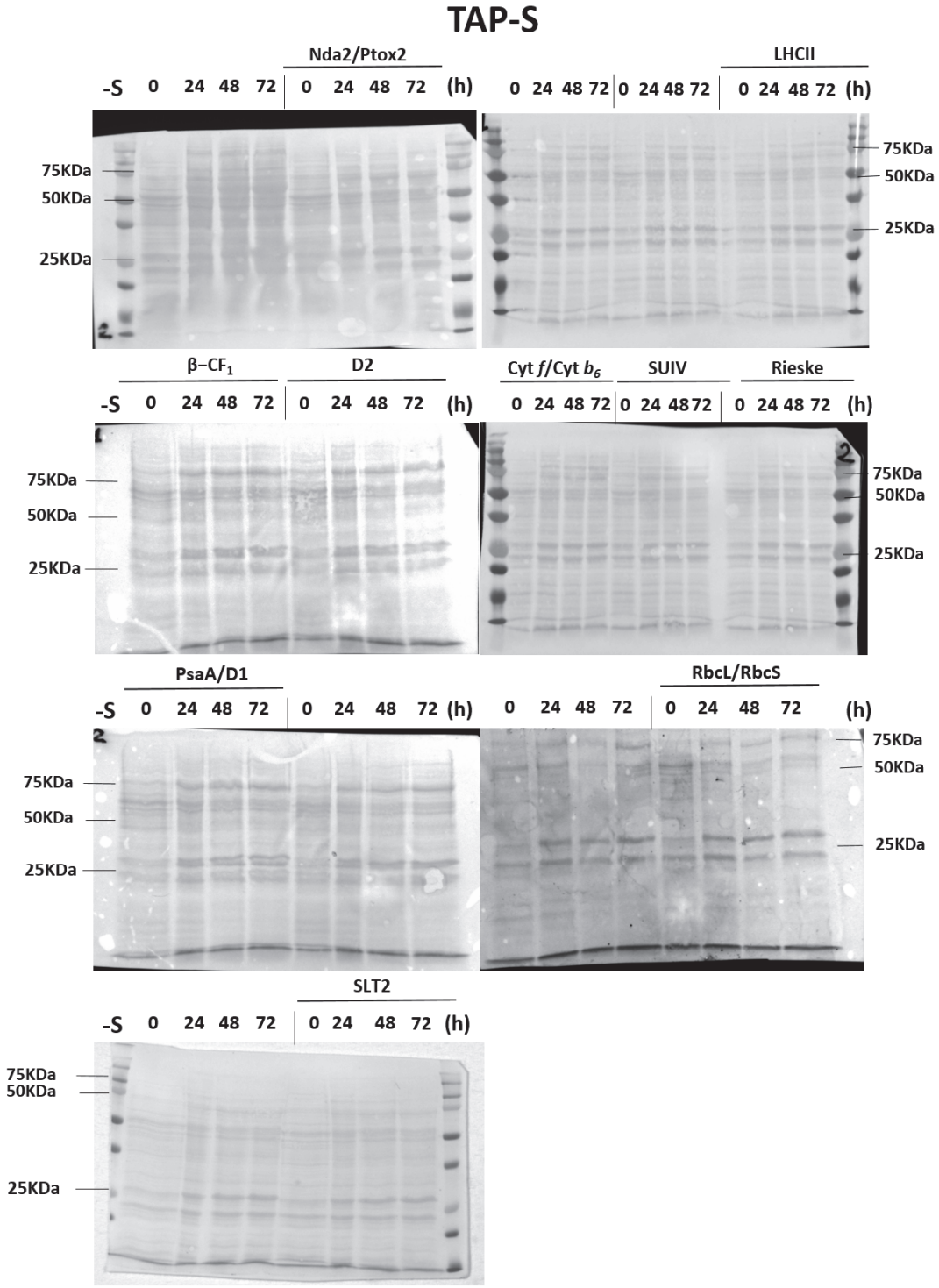

Supplemental Figure S3A. Protein loading control with Ponceau red staining for TAP-S.

One set of nitrocellulose membranes was used to assemble figure 1 (TAP-S medium) and stained with Ponceau red to verify correct gel loading. Gels were loaded on a chlorophyll content basis. For chlorophyll concentration determination, optical density at 680 nm was determined. 3–5 µg of chlorophyll was typically loaded per lane. The proteins probed in figure 1 are indicated for each membrane.

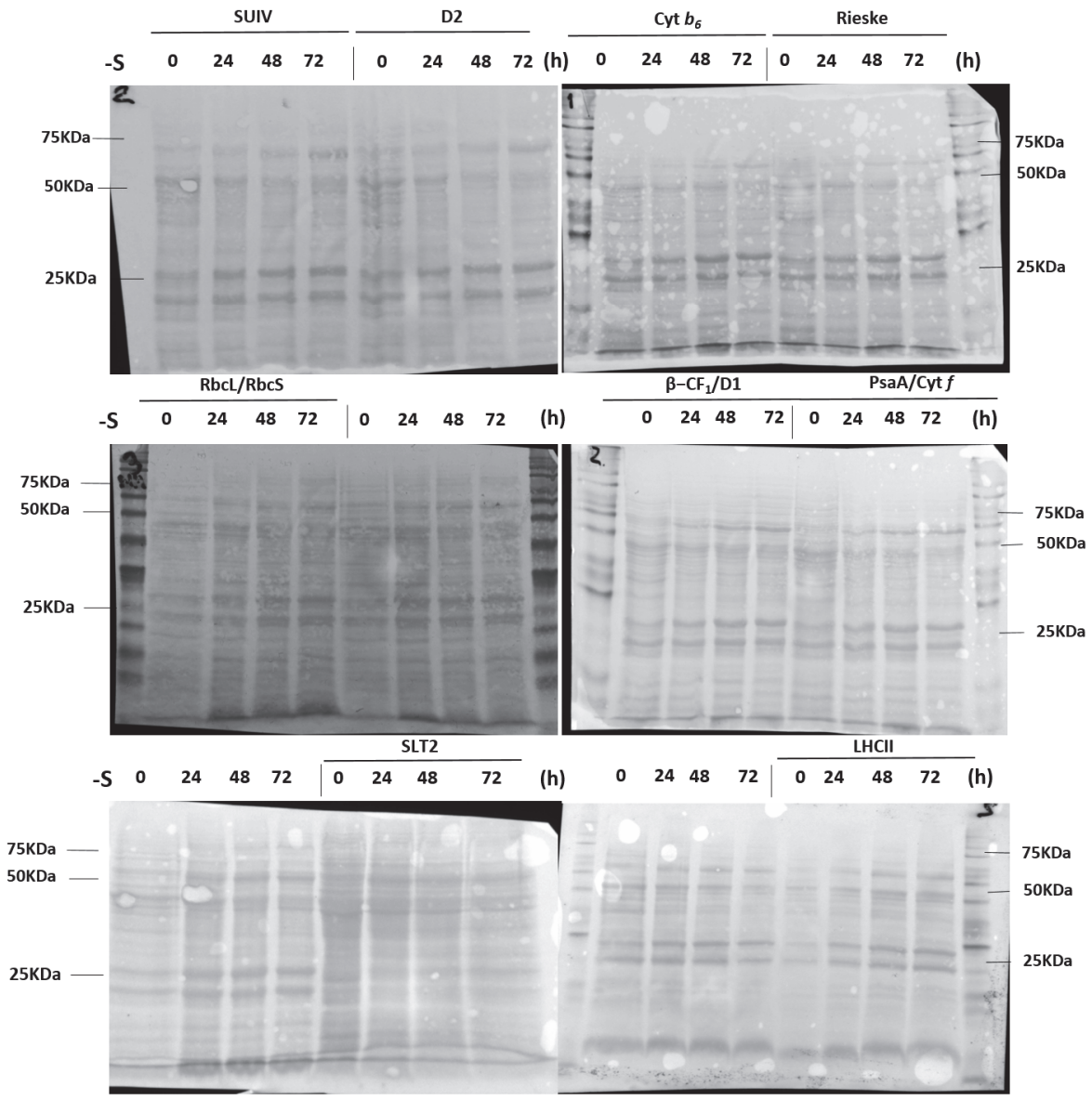

Supplemental Figure S3B. Protein loading control with Ponceau red staining for M.M.-S.

One set of nitrocellulose membranes was used to assemble figure 1 (minimal medium, M.M.-S) and stained with Ponceau red to verify correct gel loading. Gels were loaded on a chlorophyll content basis. For chlorophyll concentration determination, optical density at 680 nm was determined. 3–5 µg of chlorophyll was typically loaded per lane. The proteins probed in figure 1 are indicated for each membrane.

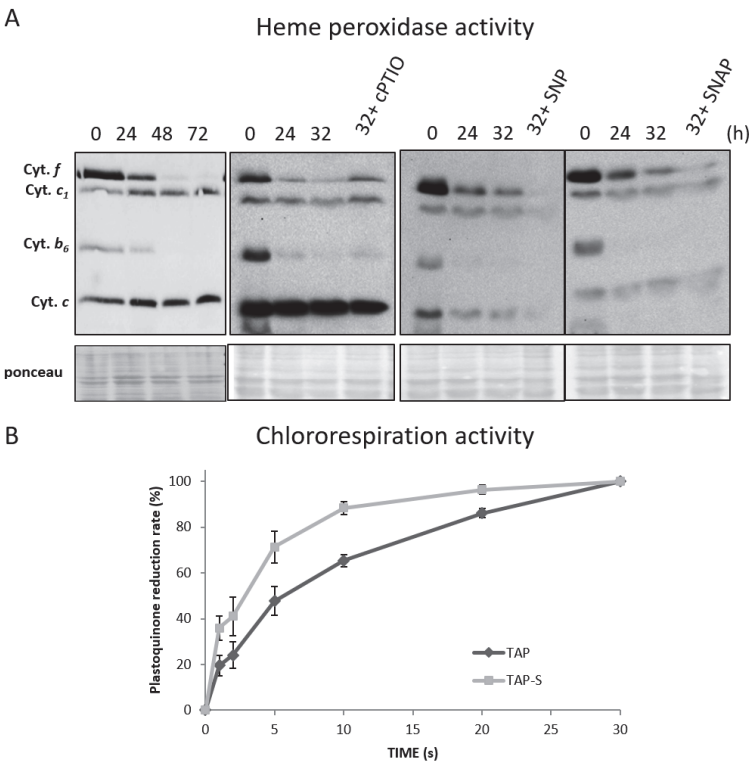

Supplemental Figure S4: Respiratory metabolism and chlororespiration

(A) Peroxidase activity of heme c groups from total extracts of WT-S24 starved in heterotrophy. The peroxidase activity was assessed as in Vargas et al. (1993) at the time points indicated in the absence or presence of NO donors (either SNP or SNAP) or of the NO scavenger cPTIO.

(B) Chlororespiratory activity of ΔpetA cells in TAP and in TAP-S after 48 h of starvation. Measurements were taken as described in (Houille-Vernes et al., 2011). Results show the mean of three independent experiments ±SEM. Data were normalized to F_M under TAP conditions.

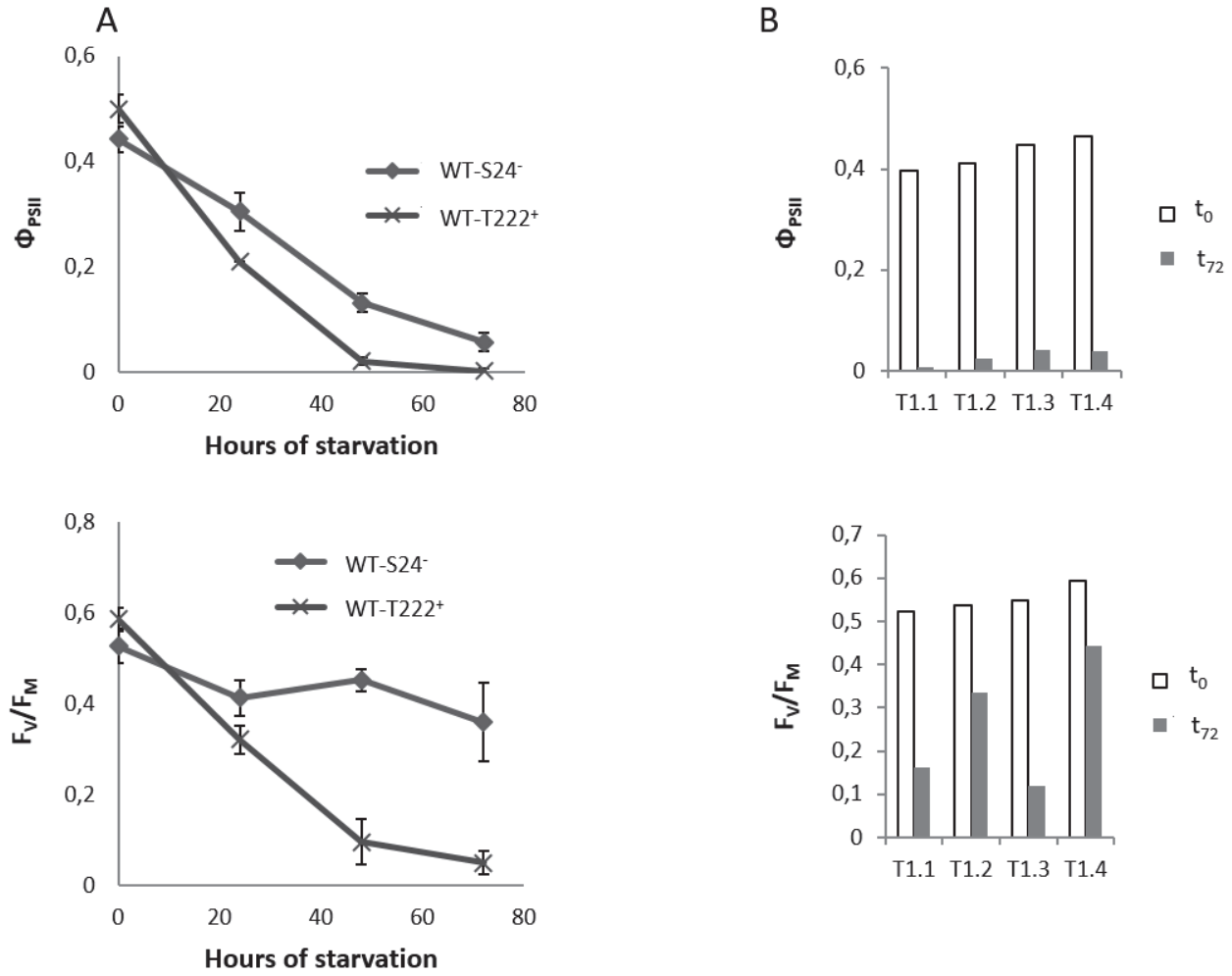

Supplemental Figure S5. Effects of sulfur deprivation in darkness and in heterotrophy on WT-S24$^-$ and WT T222$^+$.

(A) The evolution of Φ_{PSII} and F_V/F_M during sulfur starvation of strain WT-S24$^-$ (diamonds), and WT T222$^+$ (crosses) in TAP-S and complete darkness. Data represent the mean of three independent experiments ±SEM.

(B) The evolution of Φ_{PSII} and F_V/F_M of one representative tetrad obtained from crossing of WT-S24$^-$ and WT T222$^+$.

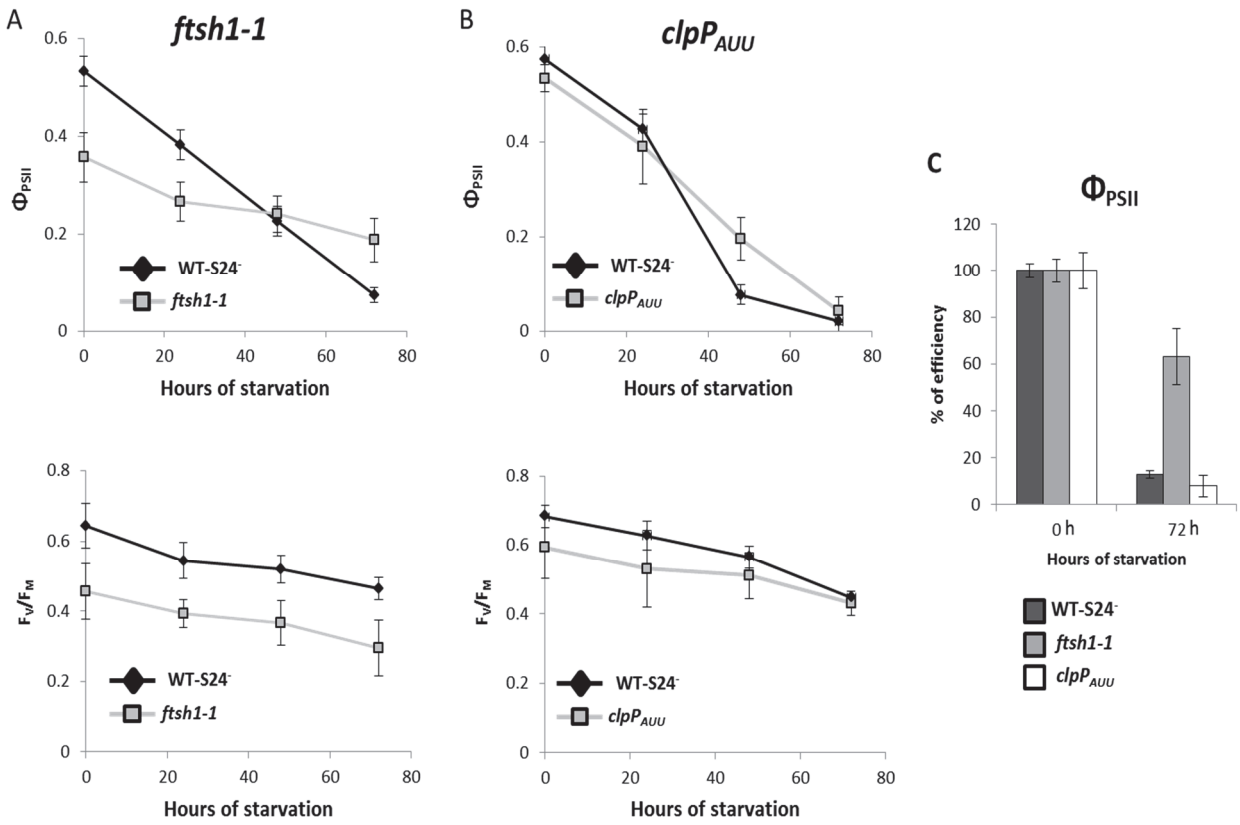

Supplemental Figure S6. Sulfur starvation in the *ftsh1-1 and clpP$_{AUU}$* mutants, defective for protease function.

(A) Comparison of the evolution of the photosynthetic parameters, Φ_{PSII} (top) and F_V/F_M (bottom), for WT-S24 and *ftsh1-1* under starvation in TAP-S and 15 $\mu E \cdot m^{-2} \cdot s^{-1}$.

(B) Comparison of the evolution of the photosynthetic parameters, Φ_{PSII} (top) and F_V/F_M (bottom), for WT-S24$^-$ and *clpP$_{AUU}$* under starvation in TAP-S and 15 $\mu E \cdot m^{-2} \cdot s^{-1}$.

(C) Residual photosynthetic efficiency (as a % of the initial efficiency) after 72 h of starvation between WT-S24$^-$, *ftsh1-1* and *clpP$_{AUU}$*.

Data represent the mean of five independent experiments ± SEM.

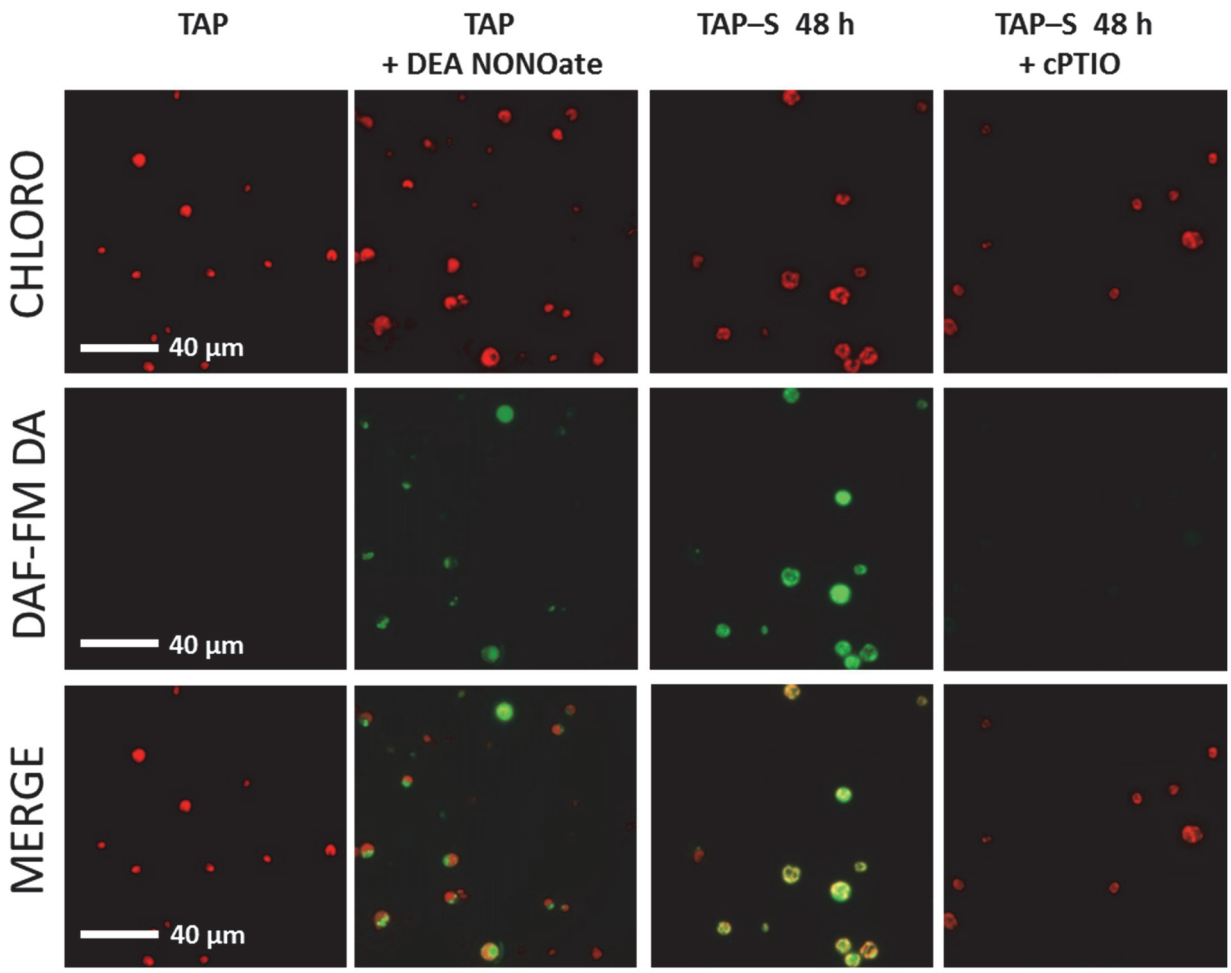

Supplemental Figure S7. DAF-FM DA fluorescence can be seen only in the presence of NO or under sulfur starvation.

Visualization of NO production *in vivo,* using the DAF-FM DA (5 µM) probe. Cells were harvested and observed with a fluorescence microscope after a washing step and 10-fold concentration. CHLORO, chlorophyll autofluorescence; DAF-FM DA, NO-dependent green fluorescence; MERGE, chlorophyll and NO-dependent signals visualized simultaneously.

From left to right: cells in replete medium; cells in replete medium incubated with DEA NONOate (0.1 mM); starved cells after 48 h; starved cells after 48 h incubated 1 h with NO-scavenger cPTIO (0.2 mM).

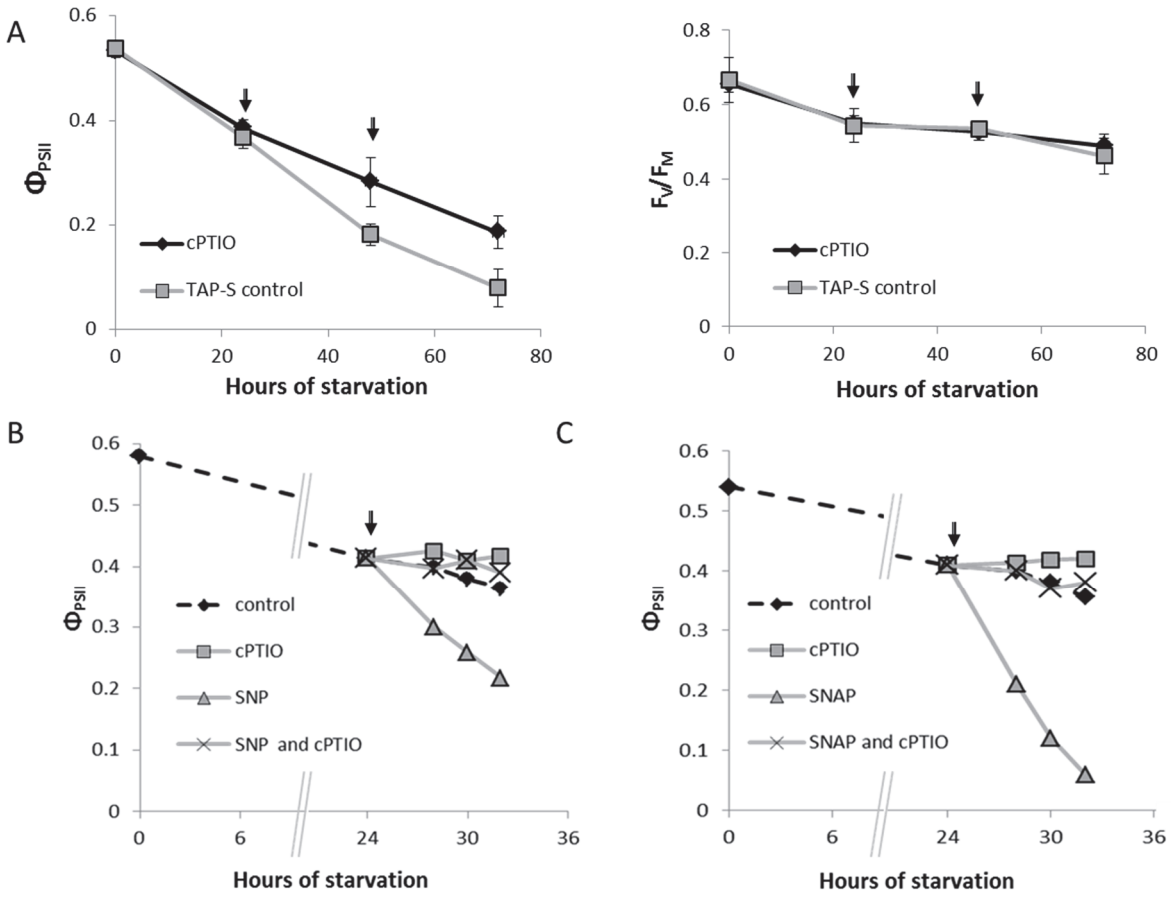

Supplemental Figure S8. Effects on photosynthetic parameters of cPTIO alone or in the presence of NO donors.

(A) Φ_{PSII} and F_V/F_M evolution measured after addition of cPTIO (0.1 mM) every 24. Data show the mean of three independent experiments ± SEM.

(B) Effects on photosynthetic efficiency of SNAP (0.05 mM) and cPTIO (0.2 mM), added alone or together.

(C) Effects on photosynthetic efficiency of SNP (0.5 mM) and cPTIO (0.2 mM), added alone or together. Black arrows indicate drug addition, experiments were performed in TAP-S at 15 $\mu E \cdot m^{-2} \cdot s^{-1}$.

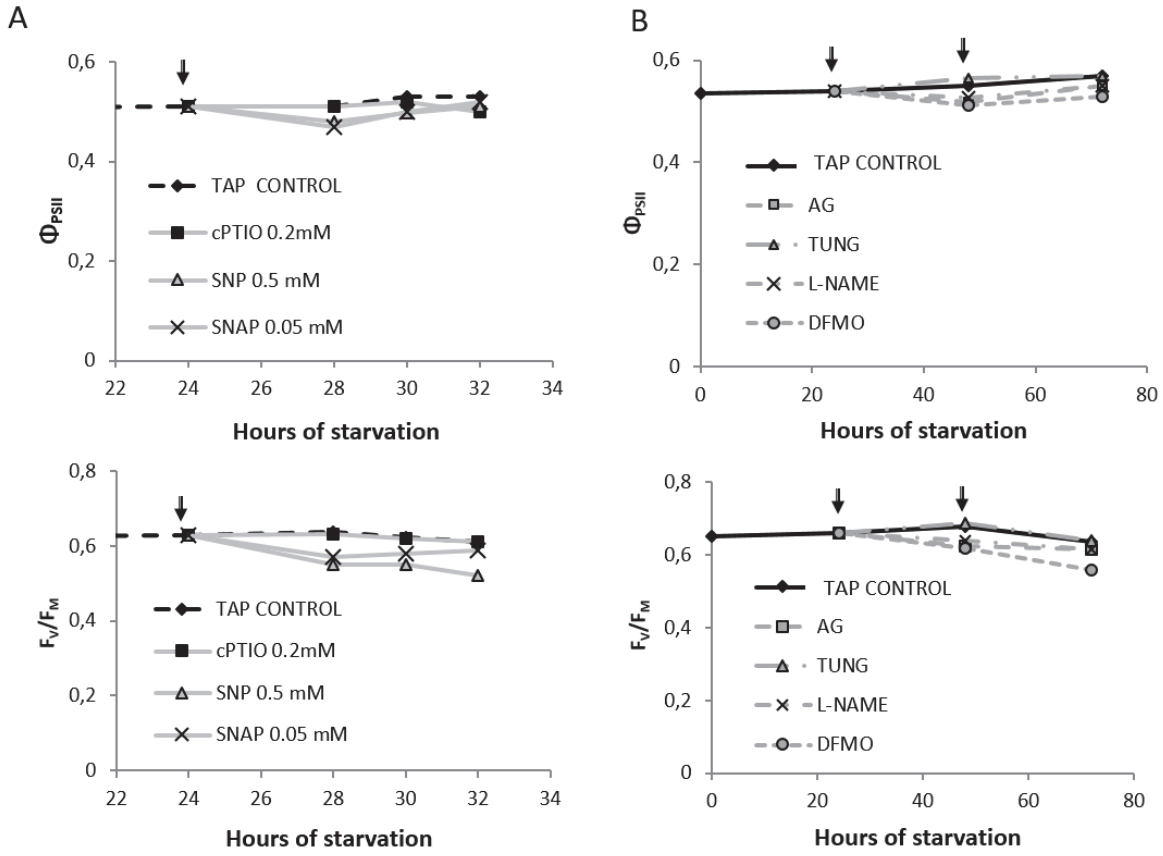

Supplemental Figure S9. Effects of NO donors/scavenger and NO synthesis inhibitors on photosynthetic parameters in sulfur-replete conditions.

(A) Effects of NO scavenger/donors on Φ_{PSII} (top) and F_V/F_M (bottom) of WT-S24$^-$ cells kept in TAP at 15 $\mu E \cdot m^{-2} \cdot s^{-1}$.

(B) Effects of NO synthesis inhibitors (1 mM final concentration for all) on Φ_{PSII} (top) and F_V/F_M (bottom) of WT-S24$^-$ cells kept in TAP at 15 $\mu E \cdot m^{-2} \cdot s^{-1}$.

Arrows indicate the addition of drugs.

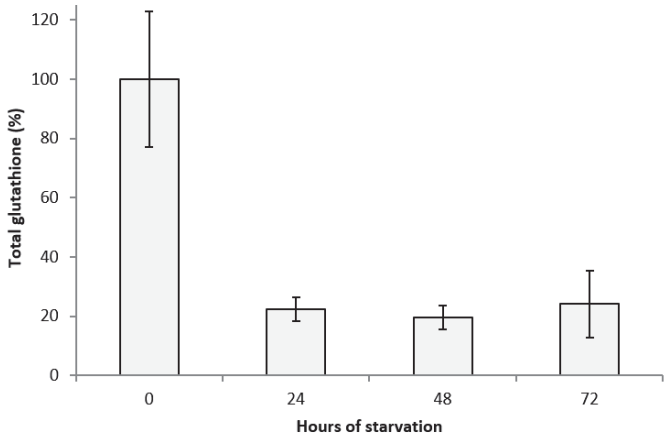

Supplemental Figure S10: Total glutathione content of cell extracts during sulfur starvation

Samples were harvested at the times indicated during sulfur starvation in TAP-S and analyzed as described in (Queval and Noctor, 2007) and (Pérez-Martin et al., 2014). Data represent the mean of three independent experiments ±SEM.